Surface abundance distribution and radial velocity pulsations in roAp star HD 24712

T.A. Ryabchikova[a,b], V.V. Tsymbal[c], V.P. Malanushenko[d], I.S. Savanov[d]

[a] **Institute of Astronomy, Russian Academy of Sciences, Pyatnitskaya 48, 109017 Moscow, Russia**
[b] **Visiting scientist, Institute for Astronomy, Vienna University**
[c] **Tavrian National University, Simferopol, Crimea, Ukraine**
[d] **Crimean Astrophysical Observatory, Isaac Newton Institute of Chile, Crimean Branch, 334413 Nauchny, Crimea, Ukraine**

Abstract. We present the abundance distribution of Mg, Fe, Co, Nd, Pr on the surface of the roAp star HD 24712. Co, Nd and Pr are concentrated in one big spot near the visible south magnetic pole of the star, while Mg is depleted in the same region. Intensity variations of the iron lines can be explained by the Fe abundance distribution around the magnetic equator. A search for radial velocity (RV) variations resulted in discovery of rapid RV variations in the PrIII λ 6160.24 Å line with an amplitude of 250 m s^{-1} and a period P=6.32 min. This period does not coincide with the known period, P=6.15 min, of the photometric pulsations. We did not find rotational modulation of the RV amplitude, which should be expected in an oblique pulsator model for roAp stars.

1. Introduction

HD 24712 (HR1217, DO Eri, V = 6.00) is a well-known variable, rapidly oscillating Ap (roAp) star. It possesses light (Wolff & Morrison, 1973) spectrum and magnetic (Preston, 1972) variations with a rotation period P=12.46 days. Kurtz (1981) discovered photometric oscillations with a period of 6.15 min. Later Kurtz (1982) found that the maximum of the pulsational amplitude corresponds to the maximum of the longitudinal magnetic field (B_l) which does not change polarity. Matthews et al. (1988) found radial velocity (RV) variations with an amplitude of 0.4 ± 0.05 km s^{-1} and with the main frequency of the photometric pulsations. Moreover, according to the authors the amplitude of the RV variations correlates with the amplitude of the photometric pulsations showing its maximal value at the phases of the magnetic maximum.

Additional magnetic field measurements were published by Ryabchikova et al. (1997). The authors also investigated spectral variability of HD 24712, and provided an abundance analysis of the star at the phases of the maximum and minimum of the longitudinal magnetic field. They pointed out that the rotational period P=12.4610 days obtained by Mathys (1991) from magnetic measurements removes the phase shift between light, spectrum and magnetic variations, while the rotational period P=12.4572 days obtained from photometry (Kurtz & Marang, 1987) gives a 0.08 phase shift between photometric and magnetic variations. Recent very accurate B_l measurements made by Wade et al. (1999) seem to favour the photometric period, although a special investigation is nedeed to clarify the period problem for HD 24712, which is important for establishing connection between magnetic and pulsational phenomena and surface abundance distribution.

We present the fisrt results of abundance mapping of HD 24712, and preliminary results of RV monitoring.

2. Observations and data reduction

High-speed spectroscopy of HD 24712 was performed in December 1998 - March 1999. Spectra were obtained with the Photometries CCD camera installed in the coude spectrograph of the 2.6 m Schajn reflector of the Crimean Astrophysical Observatory. The exposure time was 60 seconds. We had to use a wider slit corresponding to a resolving power of R=20000 to obtain a mean signal-to-noise ratio of about 30-60 for an individual spectrum. All observations were made in the spectral region 6110-6175 Å which contains FeI, BaII, PrIII and NdIII lines. The observational log is given in Table 1. The second and the third columns give the number of spectra per night and the duration of the observations in minutes. The last column gives the rotational phase corresponding to the middle of each observational night. The same reduction procedure as described in Savanov et al. (1999) for γ Equ RV observations was used.

Table 1: *HD 24712: journal of RV observations*

HJD 2400000+	Number of spectra	Time (min)	Phase of rotation
51177.315	39	53	0.920
51183.274	45	60	0.399
51184.293	45	62	0.480
51186.418	24	33	0.651
51197.219	22	30	0.518
51199.253	15	19	0.681
51206.286	21	28	0.246
51213.193	39	54	0.800
51221.202	32	45	0.443
51222.205	35	48	0.524
51223.210	56	89	0.604
51240.191	40	56	0.968

The spectral resolution of the Crimean spectra is not sufficient for abundance mapping of HD 24712 (see Sect.3), therefore we used for this purpose the observations described in Ryabchikova et al. (1997). These observations were carried out with the coude spectrograph of the Canada-Prance-Hawaii telescope in 1984 on eight consecutive nights, covering about 2/3 of one rotation. Spectra were obtained in the 4460-4525 Å spectral region with a 0.10 Å resolution. Crimean observations were used mainly to check abundance maps derived from CFHT spectra.

3. Abundance mapping

Ryabchikova et al. (1997) found the rotational velocity for HD24712 to be v sini=5.6 kms^{-1}. The slow rotation makes it impossible to apply usual Doppler imaging technique for mapping, because with our highest spectral resolution we have 3 resolution elements per spectral line (5-6 pixels). Therefore we used here a simplified method developed by Tsymbal. Instead of getting local abundances on the surface of the star we considered the abundance distribution as a set of circular spots with a given abundance. The following parameters define the abundance distribution which provide the best fit to the observed line profiles:

- coordinates of the center of a spot and its radius;
- element abundance inside the spot;
- element abundance in the photosphere;
- inclination of the rotational axis.

The last value, i = 137°, was taken from the magnetic geometry solution by Bagnulo et al. (1995). We used the same atmospheric parameters for the whole stellar surface as derived by Ryabchikova et al. (1997): T_{eff}=7250 K, log g=4.3, ξ_t=1.0 kms^{-1}. Our mapping procedure was applied to the elements Mg, Fe, Co, Nd whose spectral lines vary over the rotational period. It was not possible to improve the rotational period using our present observations, therefore we used here an ephemeris given by Kurtz & Marang (1987):

JD(magneticmaximum) = $2440577.^d23 + 12.^d4572$ E.

As it was pointed out in Introduction the photometric period agrees better with the most recent B^l measurements (Wade et al., 1999). The use of this period or the period from Mathys (1991) does not change significantly the main conclusions drawn in this paper. All atomic line parameters for our calculations were taken from VALD-2 (Kupka et al., 1999). For the PrIII line the oscillator strength was taken from Bord (1999).

3.1. Magnesium, cobalt and rare-earth elements

All these elements have a similar abundance distribution within one spot. As a representative of the group of rare-earth elements (REE) we choose neodymium, which has unblended lines in both spectral regions. In the red spectral region we also studied the lines of NdIII λ 6145.07, and PrII λ 6165.89, PrIII λ 6160.24. The NdIII line is blended with SiI λ 6145.02, and the PrIII line is blended with LuII λ 6159.93 and SmII λ 6160.41. Although we took these blends into account assuming the same distribution for all REE elements, the results obtained from the Nd III and PrIII lines are less confident. This is true, in particular, for the Pr distribution because the PrII λ 6165.89 line is too weak to provide a good map. Coordinates and radii of the spots and abundances in the spots and in the photosphere are given in Table 2.

Figs. 1-3 show a comparison between the observed line profiles and calculated with the adopted abundance distribution for Mg, Co and Nd. We can achieve a better fit for both Nd II lines, stronger λ 4462.98 and

Table 2: *Coordinates and radii of the spots, and abundances inside the spots and in the photosphere. The last line gives coordinates of the visible south magnetic pole*

	Coordinates(degree)		Radius	$\log(N/N_{tot})$	
Element	Latitude	Longitude	(degree)	Spot	Photosphere
Mg II	-60	30	70	-6.45	-4.65
Co II	-60	30	65	-5.05	-5.85
Pr II	-60	0	60	-9.35	-10.25
Pr III	-60	0	60	-7.46	-8.55
Nd II(blue)	-60	30	65	-8.04	-9.54
Nd II(red)	-60	30	65	-8.70	-9.30
Nd III	-60	30	65	-6.50	-7.50
South magn. pole	-68	4			

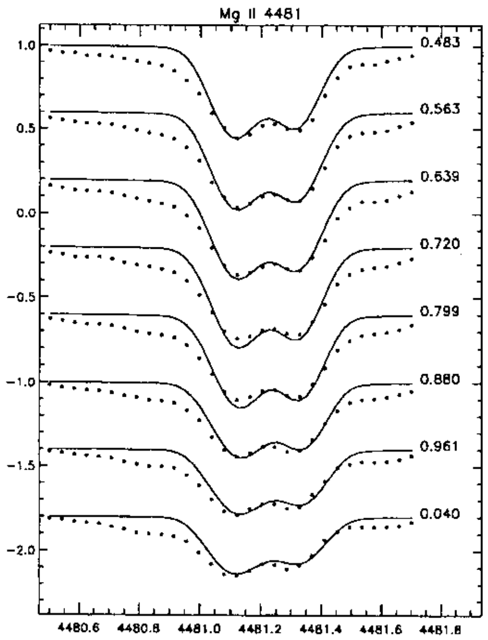

Figure 1: *Comparison of the observed (filled circles) and synthesized line profiles for Mg I λ 4481 Å using an abundance distribution from Table 2.*

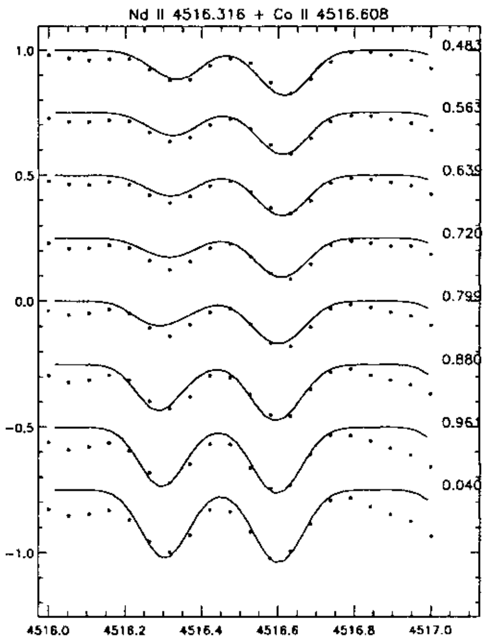

Figure 2: *The same as in Fig. 1 but for Nd II λ 4516.36 + Co II λ 4516.608 Å lines.*

weaker λ 4516.32 playing with the vertical abundance stratification, but we failed to fit NdII and NdIII lines with any unique vertical abundance distribution. This means that simple stratification cannot explain the abundance difference obtained from the lines of the first and the second REE ions.

The last line in Table 2 contains the coordinates of the visible south magnetic pole in the dipolar configuration calculated by S. Bagnulo (private communication). He used measurements of the longitudinal magnetic field by Preston (1972), and by Ryabchikova et al. (1997), as well as broad-band linear polarization measurements by Bagnulo et al. (1995). Calculations were made for the rotational period P=12.4572 days derived from photometry. The inclination of the rotational axis (i = 131°) in the new model coincides within a few degrees with that used by us. The position of the spots of Mg (depleted), Co, Nd, Pr, (enhanced) roughly coincides with the position of the visible magnetic pole. Period uncertainties may be responsible for the difference in longitudes of the spots and of the magnetic pole.

The accuracy of the spot's radius is about 10%.

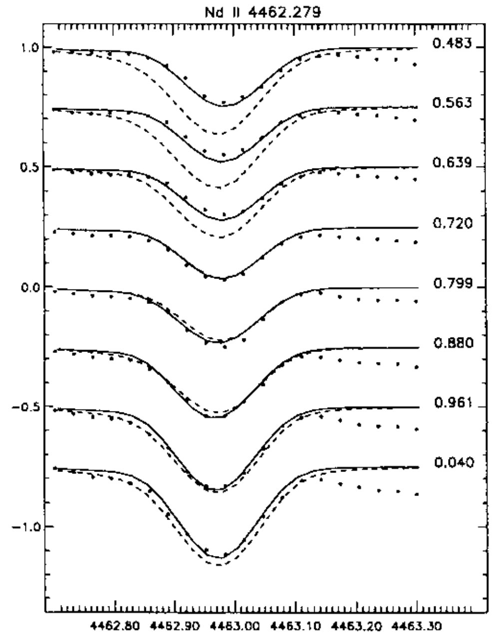

Figure 3: *The same as in Fig. 1 but for NdII λ 4462.979 line. Synthetic spectrum calculations with the spot latitude $\phi = -55°$ are shown by dashed line; those with $\phi = -60°$ are shown by full line.*

The accuracy of longitude is ±10°. The error in latitude is less certain. The calculations with the spot latitude ϕ = -55° are shown in Fig.3 by the dashed line. Note that the calculations with the spot latitude ϕ = —55° fully coincide with those for ϕ = —65°. Therefore in Table 2 we give the upper limit, $\phi \leq$ -60°. We also checked the REE distribution with 2 spots at both magnetic poles. We reject the possibility of two symmetric spots of equal abundances; a spot near the invisible magnetic pole in a dipole configuration must be less anomalous.

3.2. Iron

According to Preston (1972) and Ryabchikova et al. (1997) the iron lines vary in counter phase with the REE lines. The amplitudes of these variations are smaller. This type of variations can be successfully represented by a ring-like iron distribution around the magnetic equator. We approximated the equator band by 5 spots with R=40° each. Coordinates and Fe abundances in the spots and in the photosphere for blue spectra are given in Table 3. In red spectra the FeI λλ 6137-38 line profiles can be successfully fitted with the abundance log(Fe/**Ntot**)=-5.03 in the ring and with log(Fe/**Ntot**)=-5.35 in the photosphere. Note small abundance gradients between the equator belt and other parts of the stellar surface. The fit of the calculated line profiles to the observed ones for the blend of FeI + FeII lines at λ 4461.6 is shown in Fig.4.

Table 3: *Coordinates of the Fe spots forming a ring-like structure around magnetic equator, Fe abundances inside the spots and in the photosphere as derived from blue spectra are given.*

	Coordinates(degree)		$\log(N/N_{\rm tot})$	
Spot	Latitude	Longitude	Spot	Photosphere
1	30	31	-5.3	-5.5
2	5.7	111	-5.1	-5.5
3	-28.5	191	-4.9	-5.5
4	-16.1	271	-5.1	-5.5
5	23.9	351	-5.3	-5.5

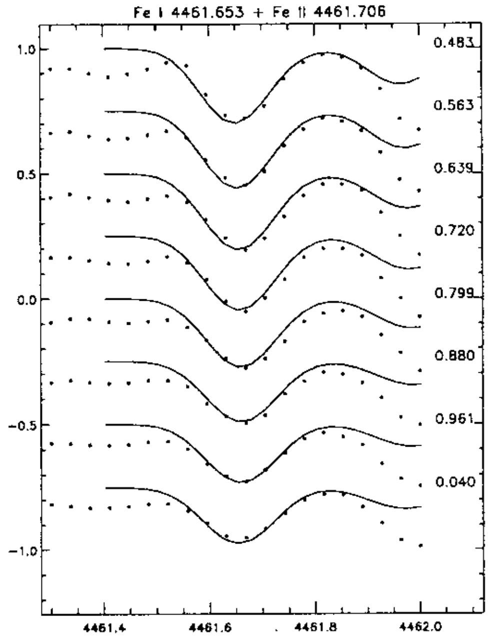

Figure 4: *Comparison of the observed (filled circles) and synthesized line profiles for FeI λ 4461.653 + FeII λ 4461.706 Å using an abundance distribution from Table 3.*

4. Rapid radial velocity variations

Savanov et al. (1999) found the highest amplitude of RV variations in the PrIIIλ 6160 and NdIIIλ 6145 lines in the roAp star γ Equ. The FeI and BaII lines did not show RV variations beyond the error limit which was estimated as 140 - 180 m s^{-1}. Due to the

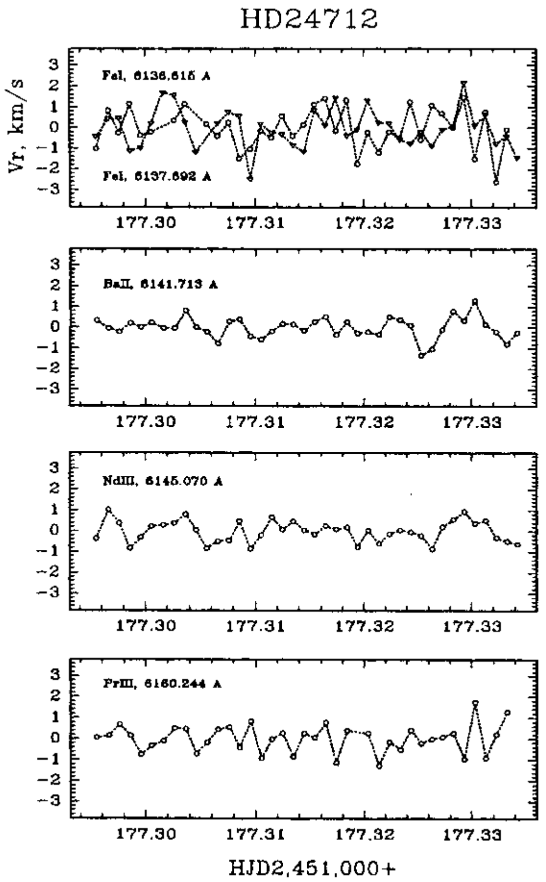

Figure 5: *Radial velocity variations obtained from Fe I, Ba II, Nd III and Pr III lines at HJD=2451177.296.*

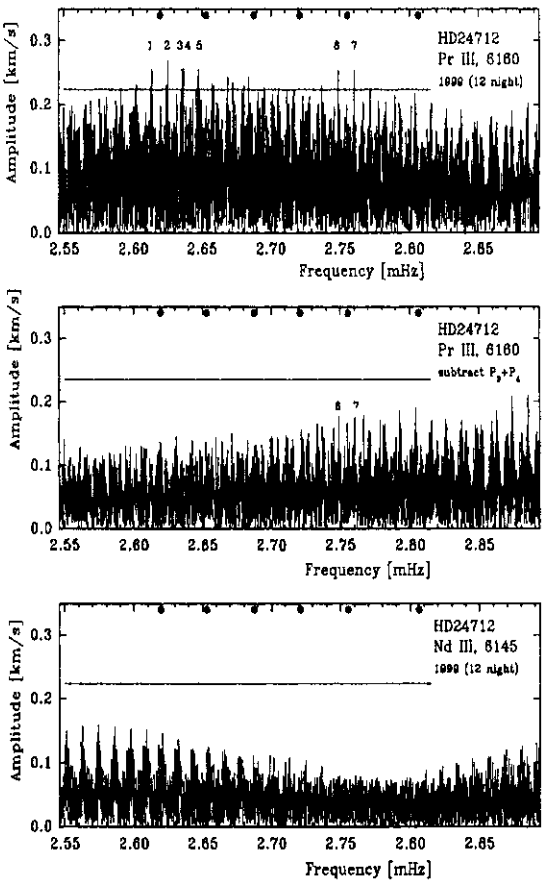

Figure 6: *Power spectrum obtained from Pr III (upper panel) and Nd III (lower panel) RV measurements. Photometric frequencies are shown by dots. Power spectrum after subtraction of the f_3+f_4 frequencies is shown in the middle panel. RV error level is given by dotted line.*

lower S/N of the present observations and lower resolving power, we get larger errors of RV measurements. We estimate them to be 200 - 400 $m\,s^{-1}$ for deeper lines (BaII, NdIII, PrIII) and 400-550 $m\,s^{-1}$ for Fe I lines. An example of the RV variations for one of the nights is shown in Fig.5.

A search for period was performed with the package ISDA (Pelt, 1992) and with the programme PERDET (Breger, 1990) in the frequency region from 2.5 mHz to 2.9 mHz, where the main photometric frequencies are observed. A power spectrum obtained from the whole observational run is shown in Fig.6 for PrIII (upper panel) and NdIII lines (lower panel). Six photometric pulsational frequencies (Kurtz et al., 1989) are indicated by the dots. Taking into account our error estimates shown by the dotted line, we conclude that marginal pulsations are registered in the Pr III line only. From seven frequencies with amplitudes exceeding the error limits, only two frequencies, f_3=2.6366 mHz (P_3=6.3213min, semiamplitude=244 $m\,s^{-1}$), and $\mathbf{f_4}$=2.6353 mHz (P_4=6.3243min, semiamplitude=160 $m\,s^{-1}$) may be considered as independent; the other frequencies are daily aliases.

Fig. 6 (upper panel) shows the positions of all 7 frequencies, while in the middle panel a power spectrum after subtraction of the signal with $\mathbf{f_3+f_4}$ frequencies is given. The pulsational period, P=6.32min, obtained from the PrIII λ 6160.24 line does not coincide with any of the photometric pulsational periods (Kurtz et al., 1989). Of course, this has to be confirmed on the basis of more accurate high-speed spectroscopic observatons.

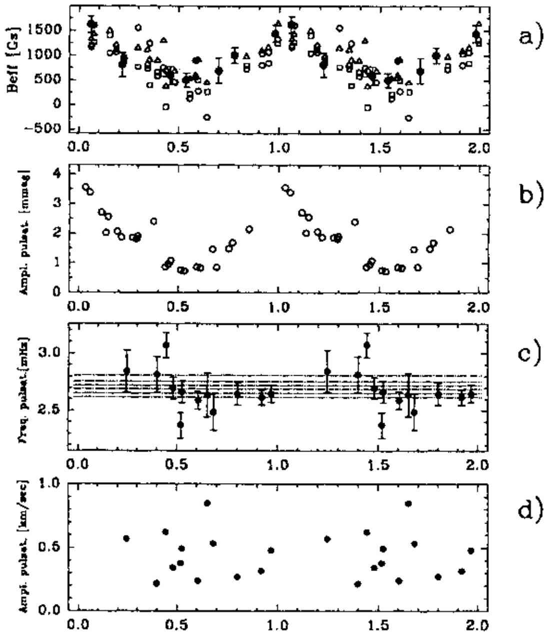

Figure 7: *Variations with the rotational period of the longitudinal magnetic field (a), photometric pulsational amplitude (b), RV (Pr III) pulsational frequency (c) and amplitude (d). Photometric frequencies in (c) are shown by dotted lines. Magnetic measurements (Mg – open circles, TiCrFe – open squares, EuGd – open triangles) are taken from Preston (1972) and from Ryabchikova et al. (1997) – filled circles.*

5. Discussion

According to the oblique pulsator model for roAp stars (Kurtz, 1982), pulsations are more effective along the magnetic axes. Photometric pulsations of HD 24712 support this model; they have the highest amplitude at the phase of passage of the south magnetic pole. Given the obtained REE abundance distribution we would expect a rotational modulation of the RV amplitudes. Fig. 7 shows variations of the magnetic field (a), photometric pulsational amplitudes (b) (Kurtz, 1982), RV (PrIII) pulsational frequencies (c) and amplitudes (d) with the rotational period. We did not find such a modulation. The accuracy of the present RV measurements does not allow one to exclude the existence of this kind of modulation with lower amplitudes. It is not unlikely that the rotational modulation exists, but its amplitude does not exceed 2 σ.

Nothing can be said concerning phase correlations, because the photometric and RV observations are spaced by 18 years, the latest longitudinal magnetic field observations shown in Fig. 7a were made 15 years ago. Period uncertainty may cause a phase shift of up to 0.1.

Acknowledgements. We thank Stefano Bagnulo who provided us with a magnetic model calculated with the photometric period. This research was supported by the Austrian Fonds zur **Förderung** der wissenschaftlichen Forschung (project *S7303-AST)* and the Russian Foundation for Basic Research (grant *98-02-16734)-*

References

Bagnulo S., Landi DegPInnocenti E., Landolfi M., Leroy J.L., 1995, Astron. Astrophys., 295, 459

Bord D.J., 1999, Astron. Astrophys., submitted

Breger M., 1990, Communications in Astroseismology, No.6

Kupka F., Piskunov N., Ryabchikova T.A., Stempels H.C., Weiss W.W., 1999, Astron. Astrophys. Suppl. Ser., 138, 119

Kurtz D.W., 1981, Inform. Bull. Var. Stars, 1915, 1

Kurtz D.W., 1982, Mon. Not. R. Astron. Soc, 200, 807

Kurtz D.W., Marang F., 1987, Mon. Not. R. Astron. Soc, 229, 285

Kurtz D.W., Matthews J.M., Martinez P., Cropper M., Clemens J.C., Kreidl T.J., Sterken C, Schneider H., Weiss W.W., Kawaler S.D., Kepler S.O., 1989, Mon. Not. R. Astron. Soc, 240, 881

Mathys G., 1991, Astron. Astrophys. Suppl. Ser., 89, 121

Matthews J.M., Wehlau W.H., Walker G.A.H., Yang S., 1988, Astrophys. J., 324, 1099

Pelt J., 1992, Irregulary Spaced Data Analysis, User manual, Helsinki

Ryabchikova T.A., Landstreet J.D., Gelbmann M.J., Bolgova G.T., Tsymbal V.V., Weiss W.W., 1997, Astron. Astrophys., 327, 1137

Savanov I.S., Malanushenko V.P., Ryabchikova T.A., 1999, Astronomy Letters, 25, No.12, 916 (in Russian)

Preston G.W., 1972, Astrophys. J., 175, 465

Wade G.A., Donati J.-F., Landstreet J.D., Shorlin S.L.S., 1999, Mon. Not. R. Astron. Soc, submitted

Wolff S.C., Morrison N.D., 1973, Publ. Astr. Soc. Pacific, 85, 141